Geophysical Research Letters, Vol. 20, No. 5, pp-391–394, 5 March 1993

ELASTIC WAVE ATTENUATION AND VELOCITY OF BEREA SANDSTONE MEASURED IN THE FREQUENCY DOMAIN

T. J. Shankland
Institut de Physique du Globe de Paris[1]

P. A. Johnson, T. M. Hopson
Los Alamos National Laboratory

Abstract. Using measurements in the frequency domain we have measured quality factor Q and travel times of direct and side-reflected elastic waves in a 1.8 m long sample of Berea sandstone. The frequency domain travel time (FDTT) method produces the continuous-wave (cw) response of a propagating wave by stepwise sweeping frequency of a driving source and detecting amplitude and phase of the received signal in reference to the source. Each separate travel path yields a characteristic repetition cycle in frequency space as its wave vector–distance product is stepped; an inverse fast Fourier transform (IFFT) reveals the corresponding travel time at the group velocity. Because arrival times of direct and reflected elastic waves appear as spikes along the time axis, travel times can be obtained precisely, and different arrivals can be clearly separated. Q can be determined from the amplitude vs. frequency response of each peak as obtained from a moving window IFFT of the frequency-domain signal. In this sample at ambient conditions compressional velocity V_P is 2380 m/s and Q_P is 55.

Introduction

Ordinarily, elastic wave travel time comes from direct measurements of transmission times between a pulse source and a receiver. Direct travel time can be difficult to measure because first-arriving energy is often emergent, i.e., slowly rising. This problem occurs particularly in heterogeneous materials such as rocks where complex, slightly different paths are available to distort wavefronts and introduce path dispersion. Other problems with directly measured travel times can include low signal to noise (*s/n*) ratios in attenuating media and distinguishing arrivals that overlap as a result of refraction, reflection, and scattering. Even interference methods such as pulse-echo overlap are commonly analysed in the time domain. The alternative approach described here, which requires controllable sources, avoids most of these problems by using time-averaged data collected wholly in the frequency domain; it is not a Fourier-transformed time-domain signal. Although this technique became apparent to us as a result of frequency domain measurements of nonlinear elastic properties in which nonlinear interactions filtered out all but one frequency (Johnson et al., 1991), the method of frequency domain reflectometry has been independently developed in radar (Isuka and Freundorfer, 1983) and optics (Ghafoori-Shiraz and Okoshi, 1986; Shadaram and Hippenstiel, 1986; Vanhamme, 1990).

[1]Now at Los Alamos National Laboratory

Method

Figure 1 is a simplified schematic diagram of an acoustic wave transmission experiment. The driving transducer receives a reference signal of the form

$$\Psi_{ref}(\omega, t) = A_{ref} \cos(\omega t) \qquad (1)$$

where angular frequency $\omega = 2\pi f$ and f is frequency. If we consider a single travel path along the vector $\mathbf{L}_i$ having length L_i, the signal received by the detector is

$$\Psi_{sam}(\omega, t) = A_i(\omega, L_i)\, e^{-\pi f L_i/Qv} \cos(\omega t - \mathbf{k}\cdot\mathbf{L}_i) = A_i(\omega, L_i)\, e^{-\pi f T_i/Q} \cos(\omega t - \omega T_i) \qquad (2)$$

where $\mathbf{k}$ is wave vector of magnitude $2\pi/\lambda$, λ is wavelength, v can be compressional, shear, or surface wave velocity, and travel time $T_i = L_i/v$. At each frequency step a transmitted (or reflected) signal can be detected with respect to the reference frequency, for instance, by a lock-in amplifier. In the high frequency range of hundreds of kHz for these experiments our detector was an electronic multiplier. If we neglect beam pattern and amplitude changes in the transducer, the product of the reference signal (1) and the phase-delayed signal (2) is a voltage that can be written in the form of sum and difference frequencies

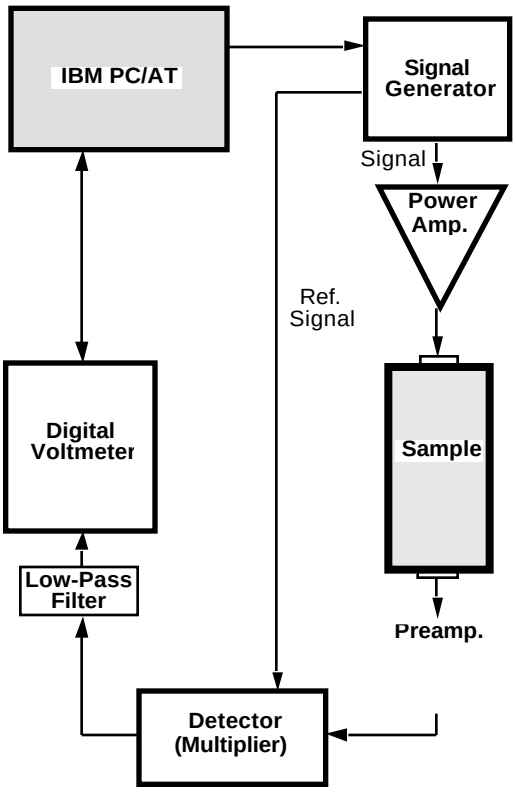

Fig. 1. Experimental configuration. The computer controls signal duration, time delays, and signal averaging in the digital voltmeter, and it stores voltage output from the DVM. Possible travel paths in addition to direct transmission include side wall reflections and surface waves.

$$V = K\frac{A_{ref}A_i}{2}\, e^{-\pi f T_i/Q} [\cos(2\omega t - \omega T_i) + \cos(\omega T_i)]$$

where K is a constant incorporating preamplifier and multiplier characteristics. Low-pass filtering plus time-averaging in the digital voltmeter (DVM) eliminates the first term in (3), and only the second, dc term remains. Incrementing frequency in steps δf increments $\mathbf{k}\cdot\mathbf{L}_i = \omega T_i$ produces a response in the frequency domain that has a characteristic periodicity $\Delta f_i = 1/T_i$ (Johnson et al., 1991). It should be pointed out that T_i contains the time delays across the transducers as well as any electronic delays, but these delays can be compensated for if the reference signal also passes through similar transducers and preamplifiers (Johnson et al., 1992), as was done for this experiment.

In practice, a received signal can contain a number of possible transmission/reflection paths L_i between source and detector. A plausible way to pick out each T_i is to perform an inverse fast Fourier transform (IFFT) on the frequency domain signal. Figure 2 shows the stepped frequency-domain response along the length of a Berea sandstone sample of dimensions $1829 \times 453 \times 453$ mm. Figure 3 is the corresponding IFFT. The reversed presentation may be confusing at first, i.e., the time domain response of Figure 3 has the peaks ordinarily seen in FFT frequency response curves. A singular

advantage of the FDTT method lies in this clear delineation of arrivals as peaks on the time axis

An intuitive way of interpreting an FDTT curve is as the broadband response to a source in the form of a delta function impulse (whose Fourier transform contains all frequencies). Each peak along the time axis represents an impulse that has traveled along a different path. In this interpretation a peak occurs for a maximum energy arrival and thus corresponds to the group velocity along its path. Arrivals after the first peak at 0.770 ms in Figure 3 are those of waves reflected off the sides of the sample in different modes. The direct travel time corresponds to a group velocity of 2380 m/s.

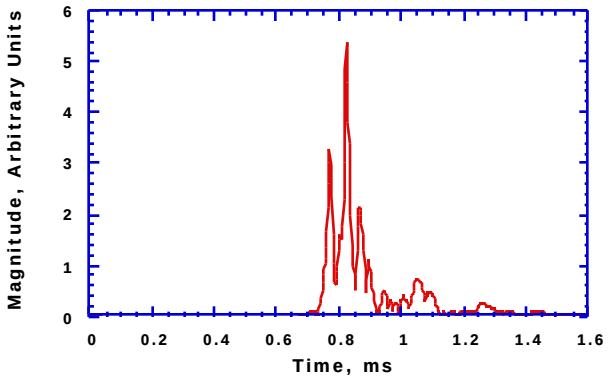

Fig. 3. Inverse Fourier transform of data from Fig. 2 showing arrival of each mode as a separate peak on the time axis.

There are several advantages to the FDTT method over simply measuring a pulse transmission time, the most obvious being the clear delineation of arrivals that would be hard to separate for transmitted pulses when different phases overlap. Even the first arrival of a pulse emerges slowly in inhomogeneous media because of wavefront distortion as different portions of the wave travel along paths of slightly different velocity. Further, time-averaging permits selectively improving *s/n* at those frequency steps where noise is a problem without having to stack an entire wavetrain. Thus, when transducers were placed side-by-side at one end of the sample, the improved *s/n* obtainable from the FDTT method permitted observation of the reflected wave off the back face of the rock, a total distance of twice the sample length or 3.66 m, although we could not detect an arrival by pulse transmission using the same apparatus (Johnson et al., 1992). We note that this configuration resembles that used in reflection seismology.

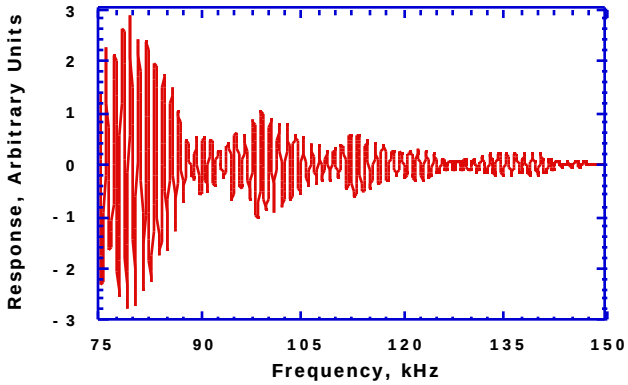

Fig. 2. Frequency domain response for first 150 kHz of a sweep from 75 to 250 kHz in steps of 50 Hz.

Conditions are imposed on this method by the properties of digital tranforms. Thus, the Nyquist sampling criterion to prevent aliasing means δf must be less than $1/(2T_{max})$, where T_{max} is the maximum travel time for which a signal is received. Time resolution $\delta T \approx 1/f_{max}$ can be improved by a wide frequency band f_{max}, but of course this requires longer measurement time.

Attenuation Measurement

From (3) we see that the amplitude of each arrival is exponentially attenuated by its travel time (equivalent to distance) and by Q^{-1}. Instead of applying an IFFT to an entire frequency domain response as done above we can apply a moving window IFFT to frequency bands within a signal such as that of Figure 2. When log(amplitude) is plotted against frequency or frequency-time product for an arrival peak, the slope yields Q for the corresponding travel path and wave mode. Figure 4 shows a moving-window transform for the largest peak of Figure 3. The remarkable *s/n* allows intensity data to be obtained over almost 4 orders of magnitude. In this case compressional wave $Q_P \cong 60$ for two different frequency sweeps having different starting and stepping frequencies. As a check on the method we also show results for a noise-free synthetic signal having Q = 60. If we include a small correction for geometrical spreading, which is inversely proportional to frequency in the far field (Pippard, 1978), the slope in Figure 4 should be steeper by an increment of log2 = 0.3 for a factor of 2 increase in frequency. Correcting for this change gives $Q_P = 55$. From differences between measurements and uncertainties about beam spreading we estimate this value to be uncertain by about ± 5.

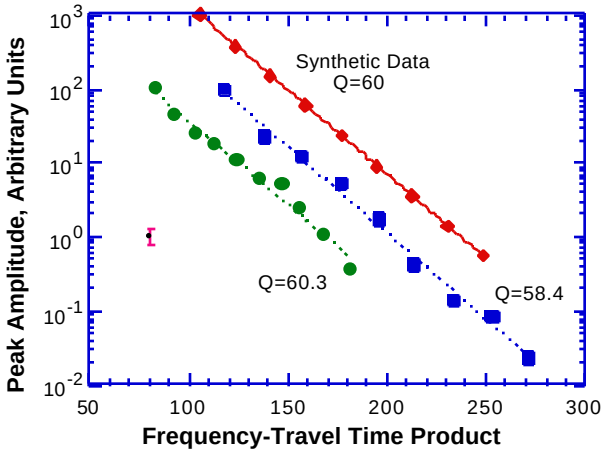

Fig. 4. Amplitude (circles) of the largest peak shown in Fig. 3 vs. frequency–travel time product as obtained from a moving window IFFT of data of Fig. 2. Also shown are results from another sweep in steps of 100 Hz from 100 to 430 kHz for the same travel path (squares) and from a synthetically generated, noise-free test signal of Q ≡ 60 (diamonds). Each window comprises 1024 points (51.2 and 102.4 kHz, respectively, for the two data sets) and overlaps 3/4 of the points in the previous window. Frequency is the mean within each window, and amplitudes are arbitrary. The error bar indicates the standard deviation of the fits to a straight line.

This Q_P is higher than values approaching 20–30 for weakly confined Berea specimens of cm-size as determined from the FFT of a pulsed arrival in almost the same frequency band (Toksöz et al., 1979; Johnston and Toksöz, 1979; Spencer, 1979; Frisillo and Stewart, 1980; Johnston and Toksöz, 1980). (Presumably, if these specimens were unconfined, their Q's would be still lower.) The value is less than 140 for Q_E of weakly confined Berea sandstone in extensional resonance in the kHz range (Winkler, et al., 1979). In comparison with unconfined specimens at ambient humidity as measured in resonance it agrees well with $Q_P \cong Q_S \cong Q_E \cong 58$ (Clark, et al., 1980) and with shear wave resonance $Q_S \cong 50$ in dry Berea sandstone (Vo-Thanh, 1990). Thus, to the extent that Berea sandstone can be assumed uniform, these results suggest an apparent variation of measured Q that depends on measurement technique such that the resonance and FDTT methods yield higher values. A possible reason is that the latter two methods have the common feature that measured intensities vary over many orders of magnitude so that corrections to measured slopes are relatively small. As a further observation, if we consider scaling with size, this very large sample can incorporate a larger range of crack sizes than can most laboratory specimens and there-

fore might be expected to have lower Q. However, there is no obvious size effect on Q, nor does it seem to vary markedly with frequency over the two orders of magnitude between the resonance and FDTT methods. We note that if there were a frequency dependence of Q and an associated velocity dispersion, then Q^{-1} would be given by the local slope on a plot such as Figure 3. Slope changes over such a limited frequency range would be hard to detect in the presence of noise.

Conclusions

For this sample, which was at ambient conditions, compressional velocity is 2380 m/s and Q_P is 55. Although only one of the modes was analyzed here, the FDTT approach permits calculation of Q for each mode that arrives, e.g, shear, compressional, or combinations produced by reflections. Other features of the FDTT method have been documented elsewhere (Johnson, et al., 1992). These include application of nonlinear elasticity to generating low frequency waves having greater propagation distances, demonstration that phase information for each arrival is obtainable, and extension to using both in-phase and quadrature signals.

In principle, with a frequency–travel time product close to the range of Figure 3 it should be possible to use the FDTT approach as an alternative to cross–correlation analysis in order to obtain two-way travel times and Q in refraction and refraction seismology where controllable sources are available, e.g., in Vibroseis® methods. Observation of multiple echoes (Johnson, et al., 1992) suggests that reverberations in room acoustics could be studied by this approach; similarly, other long-term effects such as scattering-induced codas in architectural acoustics and seismology could be treated.

Acknowledgments. A. M. Migliori and T. Bell generously provided the high frequency electronic multiplier essential to the experiments. We thank Brian Bonner for several suggestions. This work was performed under the auspices of the Office of Basic Energy Sciences–Geosciences, U.S. Department of Energy under contract W-7405-ENG-36 with the University of California. TJS thanks the Institut de Physique du Globe de Paris and the Centre National de la Recherche Scientifique for additional support and hospitality. The contents of this paper were presented in the Edward Schreiber Symposium at the 1992 Fall Annual Meeting of the AGU.

References

Clark, V. A., B. R. Tittmann, and T. W. Spencer, Effect of volatiles on attenuation (Q^{-1}) in sedimentary rocks, *J. Geophys. Res*. **85**, 925-936 (1980).

Frisillo, A. L., and T. J. Stewart, Effect of partial gas/brine saturation on ultrasonic absorption in sandstone, *J. Geophys. Res*. **85**, 5209-5211 (1980).

Ghafoori-Shiraz, H., and T. Okoshi, Fault location in optical fibers using optical frequency domain reflectometry, *J. Lightwave Technology* **LT-4**, 316-322 (1986).

Izuka, K., and A. P. Freundorfer, Detection of nonmetallic buried objects by a step frequency radar, *Proc. IEEE* **71**, 276-279 (1983).

Johnson, P. A., T. M. Hopson, and T. J. Shankland, Frequency domain travel time (FDTT) measurement of ultrasonic waves by use of linear and nonlinear sources, *J. Acoust. Soc. Am*., 92, 2842-2850 (1992).

Johnson, P. A., T. J. Shankland, and A. M. Migliori, Continuous wave phase detection for probing nonlinear elastic wave interactions in rocks, *J. Acoust. Soc. Am*. **89**, 598-603 (1991).

Johnston, D. H., and M. N. Toksöz, Attenuation of seismic waves in dry and saturated rocks: II. Mechanisms, *Geophysics* **44**, 691-711 (1979).

Johnston, D. H., and M. N. Toksöz, Ultrasonic P and S wave attenuation in dry and saturated rocks under pressure, *J. Geophys. Res*. **85**, 925-936 (1980).
Pippard, A.B., *The Physics of Vibrations*, Cambridge University Press, Cambridge, 1978.
Shadaram, M., and R. Hippenstiel, Fourier analysis of the complex envelope of the echos in an OFDR, *Applied Optics* **25**, 1083-1085 (1986).
Spencer, J. W., Jr., Bulk and shear attenuation in Berea sandstone: The effects of pore fluids, *J. Geophys. Res*. **84**, 7521-7523 (1979).
Toksöz, M. N., D. H. Johnston, and A. Timur, Attenuation of seismic waves in dry and saturated rocks: I. Laboratory measurements, *Geophysics* **44**, 681-690 (1979).
Vanhamme, H., High resolution frequency-domain reflectometry, *IEEE Trans. Instr. Meas.* **39**, 369-375 (1990).
Vo-Thanh, D., Effects of fluid viscosity on shear-wave attenuation in saturated sandstones, *Geophysics* **55**, 712 722 (1990).
Winkler, K., A. Nur, and M. Gladwin, Friction and seismic attenuation in rocks, *Nature* **277**, 528-531 (1979).

T. J. Shankland, Département des Géomatériaux, Institut de Physique du Globe de Paris, 4 place Jussieu, 75252 Paris Cedex 05, France. (Permanent address: Earth and Environmental Sciences Division, MS D443, Los Alamos National Laboratory, Los Alamos, New Mexico 84545, USA)

P. A. Johnson, T. M. Hopson, Earth and Environmental Sciences Division, MS D443, Los Alamos National Laboratory, Los Alamos, New Mexico 84545, USA

(Received November 3, 1992; accepted November 20, 1992.)

Paper number 93GL02758.